JOURNAL OF PROPULSION AND POWER
Vol. 11, No. 3, May–June 1995

Assessment of a Three-Variable Reduced Kinetic Scheme in Prescribed Turbulence

Sanjay M. Correa*
General Electric Corporate R&D Center, Schenectady, New York 12301

A chemical kinetic scheme for the combustion of complex hydrocarbon fuels is developed and assessed at conditions typical of high-intensity turbulent combustion. In the starting scheme, the fuel is assumed to pyrolyze at a global rate to CO and H_2, which subsequently are oxidized in a series of elementary steps. The reduced scheme requires three variables: the mixture fraction ξ, the fuel mass fraction Y_f, and a combined variable Y^* for CO and H_2. The oxyhydrogen radical pool is assumed to be in a state of partial equilibrium, and the CO and H_2 burn out as the radical pool decays via recombination reactions. The reduced scheme is compared with the starting scheme on combustion stability and CO/UHC emissions, in the context of the "partially stirred reactor" (PaSR) model developed earlier. The conditions are 30 atm, 1000 K inlet temperature, 2500 K equilibrium temperature (premixture equivalence ratio = 0.8), and 5 ms reactor residence time [in the perfectly stirred reactor (PSR) limit]. PaSR simulations are conducted in the range 10–1000 Hz (mixing frequency), and in each case converge to a stochastic steady state and span the plug flow reactor-PSR limits smoothly. The reduced scheme performs well on flame stability (temperature) and fuel mass fraction, but not as well on CO and H_2, because the partial equilibrium assumption breaks down under conditions where significant amounts of fuel are present. Since only three variables are needed, the scheme is computationally fast enough for use in computational fluid dynamic studies of high-intensity turbulent combustion.

Nomenclature

C_ϕ = constant in mixing model
H = particle enthalpy
h = species enthalpy
k = turbulence kinetic energy, reaction rate
M_k = molecular weight of species k
m = mass flow rate into reactor
m_p = particle mass
N_{in} = number of particles flowing in per time step
N_p = number of particles in ensemble
N_s = number of species
P = probability density function
T = temperature
t = time
V = reactor volume
W = molecular weight
w_k = molar production rate of species k per unit volume
Y_k = mass fraction of species k
Z = elemental mass fraction
ε = dissipation rate of turbulence kinetic energy
ξ = mixture fraction
ρ = density
σ = mole number
τ = reactor residence time
ω = mixing frequency

Subscripts

f = fuel
in = inlet conditions
k = index of kth species

Superscripts

a = air
e = equilibrium
f = fuel
(n) = index of nth particle
$s1$ = stoichiometric
u = unburned
$\tilde{\phi}$, $\langle\phi\rangle$ = ensemble average of any quantity ϕ

Received Aug. 21, 1993; revision received Aug. 30, 1994; accepted for publication Sept. 10, 1994.

*Manager, Combustion Program, K1-ES210, P.O. Box 8. Member AIAA.

I. Introduction

GIVEN the high cost of testing and the importance of advance sales in today's environment, the designers of combustion systems need to accurately predict the effect of design changes on parameters such as flame stability, efficiency, and pollutants.[1] These parameters are controlled by chemical kinetics and their nonlinear interactions with turbulence. Modern stochastic approaches permit inclusion of complex chemical kinetics/turbulent transport in the prevalent computational fluid dynamics (CFD) methodology.[2,3] However, kinetic schemes are not available for the oxidation of complex hydrocarbons (e.g., C_nH_m with $n \approx 10$ and $m \approx 20$) of interest in gas-turbine and other internal combustion engines, although they are available for simpler hydrocarbons.[4] Hence, kinetic issues such as flame stability and certain pollutants cannot be addressed from first principles for liquid-fueled engines. Typical semiempirical approaches use a one-step scheme for the conversion of fuel to products, or a multistep scheme that starts with an assumed pyrolysis rate for conversion of the fuel to intermediates, followed by elementary steps for oxidation of the latter. The purpose of this article is to develop a simplified scheme of the second type, and to compare it with the starting scheme under realistic aerothermal conditions. The method will be developed for premixed and nonpremixed systems, but for brevity only the performance in a premixed system will be evaluated.

Reduced schemes may be considered in a hierarchy of increasing dimensionality, where the "dimensionality" refers to the number of variables needed to describe the thermochemical system:

1) One variable, viz., ξ, with fast chemistry: There are no finite rates. This approach is useful in nonpremixed systems, where it is often adequate to assume that "mixed is burned."

2) Two variables, viz., ξ and Y_f: The sole finite-rate step is the one-step pyrolysis of fuel to CO_2 and H_2O.

3) Three variables, viz., ξ, Y_f, and a combined variable for CO and H_2: The two finite rates are one-step pyrolysis of fuel to CO and H_2, and a combination of elementary rates for the burnout of CO and H_2.

4) Four and five variables, which augment the third approach above with separate descriptions of the CO and H_2 oxidation processes.

Given the empiricism in the pyrolysis rate for complex fuels, the four- and five-variable schemes may not be worth the additional computational burden. Hence, here we will use the three-variable scheme.

To realistically assess a reduced kinetic scheme, the testbed must reproduce the microscale turbulent environment of the burner, or at least that of the CFD methodology in which the reduced scheme will be employed. To this end, the partially stirred reactor (PaSR) model has been developed for turbulent combustion. It simulates spatially homogeneous but unmixed flow, and allows complicated chemistry, e.g., Correa and Braaten[5] used it to study a 27-species/77-reaction methane oxidation scheme. The PaSR model will be reviewed briefly in Sec. IV; here we note that 1) its behavior is bounded by the perfectly stirred reactor (PSR) and the plug flow reactor (PFR), providing a set of checks on the model; 2) it provides a turbulence environment typical of highly turbulent combustors,[6] namely, those in the distributed reaction zone regime[7] rather than in the weaker laminar flamelet regime[8]; and 3) the joint velocity-scalar(s) pdf transport equation for multidimensional Monte Carlo CFD[2] degenerates to the PaSR within each computational cell.[9]

Following assessment in the PaSR over the entire range of mixing frequencies possible, a reduced scheme can be implemented in the multidimensional Monte Carlo/CFD[3] model, and those predictions can be compared with data (from "real-world" inhomogeneous flow). This approach will provide the combustor designer with a predictive methodology that has been validated, to the maximum extent, at each step.

II. Starting Scheme

Since detailed kinetic schemes for complex fuels are unavailable, as discussed above, the baseline or "starting" kinetic scheme is initiated by an irreversible global pyrolysis reaction

$$C_nH_m + (n/2)O_2 \rightarrow n\,CO + (m/2)H_2 \tag{1}$$

whose rate can be a function of the equivalence ratio; chain-branching (or "shuffle") reactions such as

$$CO + OH \leftrightarrows CO_2 + H \tag{2}$$

$$H_2 + O \leftrightarrows OH + H \tag{3}$$

$$H + O_2 \leftrightarrows OH + O \tag{4}$$

$$OH + OH \leftrightarrows H_2O + O \tag{5}$$

and recombination reactions such as

$$H_2 + M \rightarrow H + H + M \tag{6}$$

$$O_2 + M \rightarrow O + O + M \tag{7}$$

$$H + OH + M \rightarrow H_2O + M \tag{8}$$

Standard rates are used for the elementary reactions above. The performance of the starting scheme is discussed in Sec. V, in conjunction with that of the reduced scheme developed next.

III. Development of the Reduced Scheme

Multistep schemes contain too many variables (species plus enthalpy) to be tractable in CFD. Hence, the number of variables must be reduced. Since the multistep pyrolysis of lower hydrocarbons has, of necessity, already been replaced by the assumed single-step pyrolysis of the complex fuel, a good start has been made towards a reduced mechanism. In this section, partial equilibrium in the radical pool is used to further eliminate (chain-branching) steps.

For purposes of this development, we assume that "air" consists of 21% O_2 and 79% N_2, by volume, and that the initial reactants are exclusively the fuel (C_nH_m) and air. Furthermore, the only species in the system are C_nH_m, O_2, N_2, CO, H_2, CO_2, H_2O, O, OH, and H. Define $W_f \equiv (nW_C + mW_H)$ and $W_a \equiv (W_{O_2} + 3.76\,W_{N_2})$, where W_i is the molecular weight of species "i" (except that W_a is not the mean molecular weight of air). This system is described in terms of three variables: ξ, Y_f, and a composite radical pool variable Y^*. The ranges of the three variables ξ, Y_f, and Y^* follow and will show that all possible thermochemical states fall within a tetrahedron in this three-dimensional ($\xi - Y_f - Y^*$) space.

The first variable is a conserved scalar called the mixture fraction ξ, which is derived by normalizing the elemental mass fractions Z_i by the values in the fuel and airstreams:

$$\xi = (Z_i - Z_i^a)/(Z_i^f - Z_i^a) \tag{9}$$

Superscripts a and f refer to the air and fuel streams, respectively. ξ is conserved because elements are unchanged by chemical reaction; likewise, the total (chemical plus sensible) enthalpy is conserved under reaction and can be mapped into ξ:

$$\xi = (h - h^a)/(h^f - h^a) \tag{10}$$

By construction, therefore, $0 \le \xi \le 1$. The stoichiometric value of mixture fraction ξ_{s1} is

$$\xi_{s1} = W_f/[W_f + (n + m/4)W_a] \tag{11}$$

The second variable is the fuel mass fraction Y_f, $Y_f^{\min}(\xi) \le Y_f \le Y_f^{\max}(\xi)$. The upper bound is set by having all the elements present in the initial reactants, i.e., $Y_f^{\max}(\xi) = \xi$. The lower bound $Y_f^{\min}(\xi)$ is set by the availability of O_2 to convert the maximum possible amount of C to CO and H_2 (not to CO_2 and H_2O). Let this value of mixture fraction be ξ_{s2}; then $Y_f^{\min}(\xi) = 0$ if $\xi \le \xi_{s2}$, where

$$\xi_{s2} = W_f/[W_f + (n/2)W_a] \tag{12}$$

If $\xi > \xi_{s2}$, then not all the fuel can be converted to CO. The excess carbon and hydrogen remain as fuel; after simplification:

$$Y_f^{\min}(\xi) = 0, \qquad \text{if } \xi \le \xi_{s2} \tag{13a}$$

$$Y_f^{\min}(\xi) = (\xi - \xi_{s2})/(1 - \xi_{s2}), \qquad \text{if } \xi > \xi_{s2} \tag{13b}$$

The third variable is a composite Y^*, defined such that $\sigma^* \equiv \sigma_{H_2} + \sigma_{CO}$, where $\sigma_j \equiv Y_j/W_j$ is the mole number of species "j." The bounds on Y^* follow from the bounds on CO and H_2. If $\xi \le \xi_{s2}$, then there is enough O_2 to convert all the C to CO. If $\xi > \xi_{s2}$, then there is only enough O_2 to convert $(Y_f^u - Y_f^{\min}) = (\xi - Y_f^{\min})$ of C to CO. After simplification, the upper bound is obtained as

$$\sigma^{*,\max} = (\xi - Y_f)(n + m/2)/W_f$$

$$\text{if } \xi \le \xi_{s2} \text{ or if } \xi > \xi_{s2} \text{ and } Y_f > Y_f^{\min} \tag{14a}$$

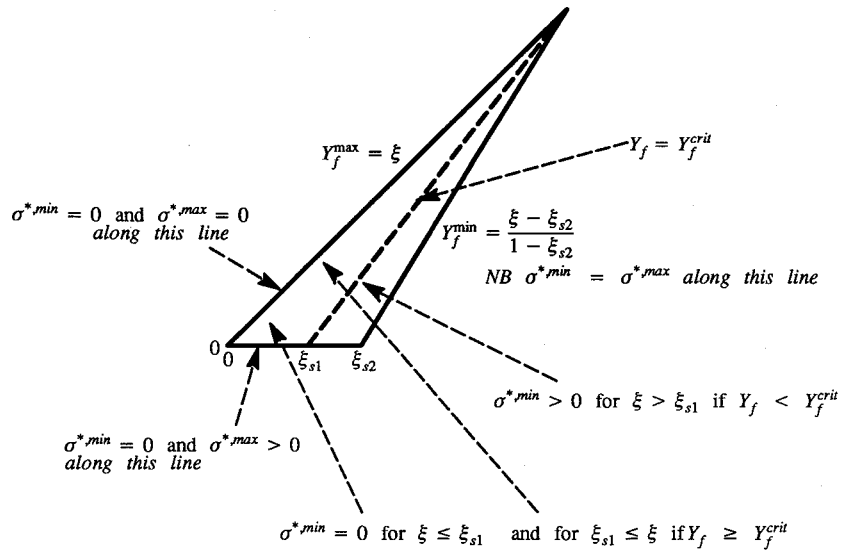

Fig. 1 Depiction of allowable $\xi - Y_f - \sigma^*$ space in $\xi - Y_f$ plane.

or

$$\sigma^{*,\max} = (1 - \xi)(2n + m)/(nW_a) \quad \text{if } \xi > \xi_{s2} \text{ and } Y_f = Y_f^{\min} \tag{14b}$$

Next, consider the lower bound $\sigma^{*,\min} \equiv (\sigma_{H_2} + \sigma_{CO})^{\min}$. For $\xi \le \xi_{s1}$, there is enough O_2 to convert all the C to CO_2 and all the H to H_2O. Hence, $\sigma^{*,\min} = 0$, for $\xi \le \xi_{s1}$. In the region $\xi \ge \xi_{s1}$ there is a critical value Y_f^{crit}, such that for $Y_f \ge Y_f^{crit}$ there is enough C and H locked up in the fuel such that the available O can convert all the remaining C and H to CO_2 and H_2O, respectively. Hence, the minimum CO and H_2 are zero. Ignoring radicals, and after algebraic simplification

$$Y_f^{crit} = \left(\frac{4W_f/W_a}{4n + m} + 1\right)\xi - \frac{4W_f/W_a}{4n + m} \tag{15}$$

If $Y_f^{min} \le Y_f \le Y_f^{crit}$, then there is not enough Y_f to lock up sufficient C and H such that the available O at that ξ can convert all the remaining C and H to CO_2 and H_2O. Hence, CO and H_2 are greater than zero, even at their minimum values:

$$\sigma^{*,min} = \xi[(2n + m/2)/W_f + 2/W_a] - [(2n + m/2)/W_f]Y_f - 2/W_a \tag{16}$$

Hence, the bounds on the three variables have been obtained. This defines the allowable region of the three-dimensional thermochemical ($\xi - Y_f - Y^*$) space in the reduced scheme. This subspace is a tetrahedron (Fig. 1). Typical values of ξ_{s1} and ξ_{s2} are 0.055 and 0.189, respectively, for CH_4; and 0.064 and 0.169, respectively, for $C_{10}H_{19.2}$ (a widely adopted model fuel).

Compared with the five-variable scheme available for CH_4,[10] the present three-variable scheme computes the radicals from partial equilibrium rather than from additional variables dedicated to the radicals. The benefit of the present approach is its computational cost savings, while the disadvantage is the loss of chemical accuracy.

In the reduced scheme, the "shuffle" reactions (2–5) are assumed to be fast enough to be equilibrated. This assumption of partial equilibrium relates the minor species to the rest of the reduced scheme. Defining the equilibrium constant of the (shuffle) reaction "M" above as K_M, and the concentration of species "i" as $(i) \equiv \bar{\rho}Y_i/W_i$, where $\bar{\rho}$ is the average density, it follows that

$$(OH) = [K_3K_4(H_2)(O_2)]^{1/2} \tag{17}$$

$$(O) = K_3K_4K_5(H_2)(O_2)/(H_2O) \tag{18}$$

$$(H) = K_3^{3/2}K_4^{1/2}K_5(H_2)^{3/2}(O_2)^{1/2}/(H_2O) \tag{19}$$

$$(CO) = [K_3K_5/K_2](CO_2)(H_2)/(H_2O) \tag{20}$$

There are 12 unknowns at each point in $\xi - Y_f - Y^*$ space: 10 mass fractions and density and temperature. The required 12 equations consist of five equations (for the enthalpy and four atomic mass fractions) from the specification of ξ; one equation from the specification of Y_f; one equation from the specification of σ^*; four equations (17–20) from the assumption of partial equilibrium; and one equation from the equation of state. These equations are nonlinearly coupled by temperature, and so an iterative method is required. The procedure was executed to produce a "look-up" table for the PaSR (reduced-scheme) simulations. The 21 × 21 × 21 grid was set nonuniformly so as to resolve the regions of large variation (e.g., the region around ξ_{s1}).

IV. PaSR Model

A testbed is required in order to compare the reduced scheme with the starting scheme.

The PaSR or "partially-stirred reactor" model may be derived formally as a subset of the joint pdf equation,[2,11] but here it is presented in physical terms. Consider a fuel-air premixture flowing into a box whose contents—reactants, products, and intermediates—are mixed by turbulence of a prescribed frequency. A steady state of "unmixedness" is maintained by the compositional difference between the inlet stream and the contents of the reactor: this is the chemical equivalent of nondecaying homogeneous turbulent flow, in which the turbulence must be maintained by external forcing. Note that the model can account for any incoming flow pdf, including the double-delta function of nonpremixed reactants. The pdf $P(Y_k)$ of mass fractions Y_k of chemical species in the reactor is represented by the N_p-member ensemble:

$$Y_k^{(1)}, Y_k^{(2)}, \ldots Y_k^{(N_p)}, \qquad k = 1, \ldots N_s$$

Each of the members $n = 1, \ldots N_p$ is referred to as a "particle."

Scalar mixing is accounted for by the so-called "interaction-by-exchange-with-the-mean" (IEM) submodel.[12] The equation for a particle is

$$\frac{dY_k^{(n)}}{dt} = -C_\phi\omega(Y_k^{(n)} - \bar{Y}_k) + w_k^{(n)}\frac{M_k}{\rho^{(n)}}, \qquad k = 1, \ldots N_s \tag{21}$$

where ω is the mixing frequency in the IEM model, $w_k^{(n)}$ is the molar production rate of species "k" per unit volume for the nth particle, and $\rho^{(n)}$ is the density of the nth particle. Thermochemical properties and the kinetic database are accounted for using CHEMKIN-II.[13] It is worthwhile to point out that Eq. (21) is solved as shown, without fractional steps, and so mixing and chemistry will be accounted for simultaneously. This avoids some of the difficulties that have been noted in other Monte Carlo mixing models.[14] The IEM term describes linear deterministic relaxation to the mean. The constant C_ϕ in Eq. (21) is set to unity to be consistent with the scalar dissipation term in the k-ε-g model.[9,15]

The corresponding equation for the particle temperature is

$$\bar{C}_p\frac{dT^{(n)}}{dt} = \frac{dH^{(n)}}{dt} - \sum_{k=1}^{N_s} h_k\frac{dY_k^{(n)}}{dt} \tag{22}$$

where $H^{(n)}$ is the total enthalpy of particle n. Hence, the PaSR is described by a coupled system of $(N_s + 1) \times N_p$ first-order ordinary differential equations (o.d.e.s) in time.

The IEM model is preferred to the Curl model,[16] which has been widely used in stochastic modeling of combustion,[17-19] for two principal reasons. It can be parallelized with nearly 100% efficiency for parallel processor computers, and it allows simultaneous mixing and chemistry that avoids kinetically inaccessible postmixing states.[14]

The algorithm proceeds as follows (Fig. 2). On each global time step, a certain number of particles N_{in} enters the PaSR; each particle has equal mass m_p

$$m_p = m\Delta t/N_{in} \tag{23}$$

where m is the mass flow rate into the PaSR. In the premixed case, the incoming particles have identical enthalpy and initial composition. Particles, which are selected randomly from the ensemble, flow out at the same mass flow rate. Since the mixing model is deterministic, it is this outflow selection process that introduces the element of randomness to the PaSR model. Particles in the ensemble evolve according to Eqs. (21) and (22). The global residence time τ in the reactor is computed for informational purposes as

$$\tau = \bar{\rho}V/m \tag{24}$$

where $\bar{\rho}$ is the mean density and V is the volume. The integration is continued until a stochastic steady state is achieved, typically for 5–10 times the mean residence time in the PaSR. From the steady-state ensemble, scatterplots and correlations of interest can be obtained.

In the case of the starting scheme, Eqs. (21) and (22) are integrated by a modified Gear's method. In the case of the reduced scheme, given its intended use in CFD codes, a cheaper method is desired, and so the equations are integrated in an explicit analytical manner as follows. Consider a variable ϕ, evolving under the influence of a chemical source term and the IEM term:

$$\frac{d\phi}{dt} = w - C_\phi\omega(\phi - \bar{\phi}) \tag{25}$$

with the initial condition $\phi = \phi_0$ at the start of the time step δt. Defining

$$a = w + C_\phi\omega\bar{\phi} \quad \text{and} \quad b = -C_\phi\omega \tag{26}$$

the solution is

$$\phi = [(a + b\phi_0)e^{b\delta t} - a]/b \tag{27}$$

This solution is implemented for each of the Eq. (25), with ϕ denoting either Y_f or Y^*, which are the reactive scalars in the reduced scheme. In Eq. (27), the chemical source term is evaluated at the beginning of the explicit integration time step. Note that this step is much smaller than the global step, i.e., $\delta t \equiv \Delta t/L$, where Δt is the global time step and L is ≈500. The size of δt is chosen to resolve the fastest chemical steps (those associated with Y^*). There are obvious ways to improve the accuracy of this approach, but at additional computational cost. For example, another approach is a priori integration of the rate terms at each $\xi - Y_f - Y^*$ point for preselected ω and Δt, using an appropriate integration technique regardless of cost, and storage of the ΔY_f and ΔY^* at that $\xi - Y_f - Y^*$ point; the PaSR (or CFD) code would interpolate directly for ΔY_f and ΔY^*, rather than for the rates and, hence, no real-time integration would be required.

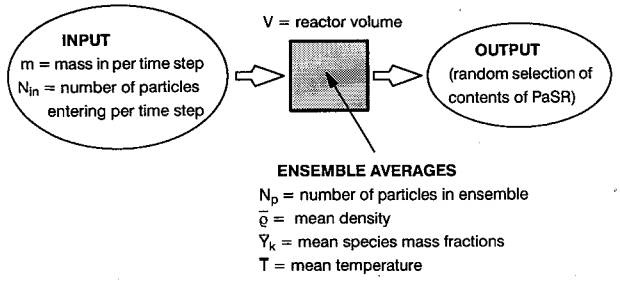

Fig. 2 Diagram showing nomenclature adopted in the PaSR model.

V. Assessment in Prescribed Turbulence

As mentioned above, since the incoming particles can have compositions and temperatures corresponding to any desired pdf, both premixed and nonpremixed systems can be accommodated in the PaSR model. However, only premixed cases are discussed here.

The PaSR was applied to premixed combustion of a hydrocarbon fuel at 30 atm and 1000 K inlet conditions. Thermodynamic properties and the C:H ratio in the fuel are taken to be those of methane, but the kinetic scheme is that given in Sec. II (starting scheme) and Sec. III (reduced scheme). The pyrolysis rate is taken to be $3 \times 10^{14}\, e^{-22{,}000/RT}$, in cm^3-s-cal-mol-K units. The rate is chosen (and could be altered to suit other purposes) to give desired results in the PSR and PFR limits. In the PSR limit, the mass flow rate and reactor volume give a residence time of approximately 5 ms. The equivalence ratio of 0.8 leads to a 1500 K equilibrium temperature rise, although it will be seen that the actual rise is kinetically limited to about half this amount. This very incomplete combustion focuses attention on the flame zone of a practical burner; the presence of large amounts of unburned fuel provides a severe test of the reduced scheme. The simulations were run for mixing frequencies of 10–1000 Hz, spanning the PFR-PSR limits (as shown below) and also covering most of the expected range of ε/k in combustors, where k is the turbulence kinetic energy and ε is the dissipation rate.[5]

The PaSR algorithm converges to a stochastically steady state for the means in about five residence times. Figure 3 shows the convergence path for the starting and the reduced schemes: the parameter is the mean temperature from the 100-Hz simulation, but the result is typical of all parameters.

Post steady-state ensemble-mean quantities obtained from the PaSR model, using the starting and the reduced schemes, are shown in Fig. 4. In each case, the independently computed high-frequency limit (PSR) and low frequency limit (PFR

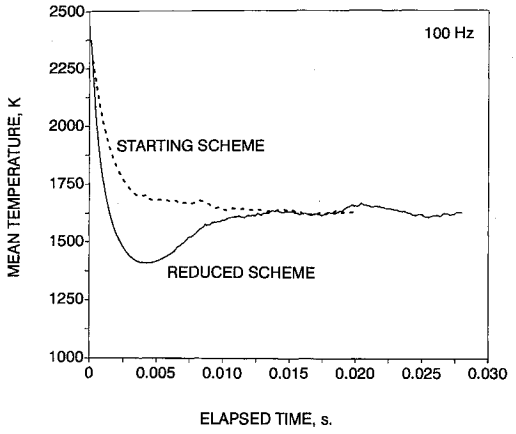

Fig. 3 Typical convergence path to stochastic steady state: ensemble-mean temperature at 100 Hz.

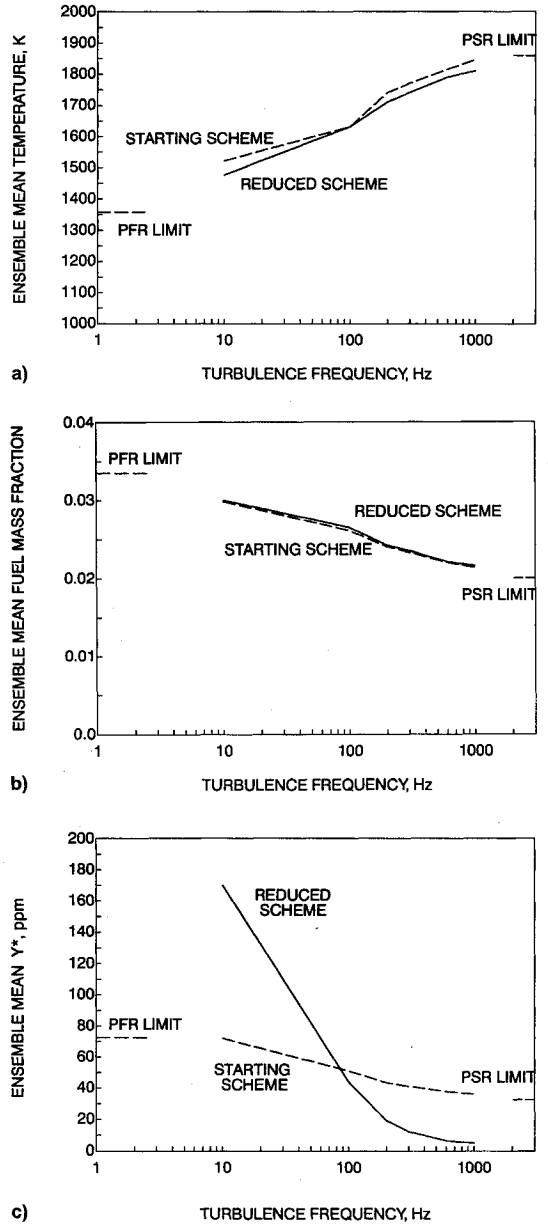

Fig. 4 Comparison of ensemble-mean quantities obtained from the PaSR model using the starting and the reduced schemes. The PFR and PSR limits were obtained using the starting scheme in independent codes: a) mean temperature, b) mean fuel mass fraction, and c) mean Y^*, combined variable based on the CO and H_2 mole numbers.

convoluted with the theoretical age distribution) are also shown. All PaSR predictions lie smoothly between these limits, providing a set of checks on the model. Several points can be made:

1) The global pyrolysis rate in the starting scheme does not yield complete combustion, appropriate for a heavy hydrocarbon under present circumstances. The low frequency limit has only a 360 K temperature rise; mixing is required to accelerate ignition of the incoming reactants, but even in the high-frequency mixing limit the PSR temperature rise is only 860 K and not the 1500 K equilibrium rise. The assumed rate can be altered to produce other results, if desired.

2) The agreement between the starting scheme and the reduced scheme is excellent on the mean temperature (Fig. 4a) and on the mean fuel mass fraction (Fig. 4b), at all frequencies from 10–1000 Hz. The agreement on fuel mass fraction is not surprising since fuel pyrolysis is explicitly recognized as a degree of freedom (DOF) in the reduced scheme. The latter is a desirable feature.

3) The agreement on mean Y^*, which is the combined variable based on the CO and H_2 mole numbers, is not as good (Fig. 4c). Potential contributors to this discrepancy are the integration error, the coarseness in the look-up table, and the assumption of partial equilibrium. These factors can be examined in turn. First, the integration time step δt is small enough ($\delta t = 0.2\ \mu s \ll 1/w^{max}$) to resolve the fastest rates in the system; in fact, simulations with smaller time steps gave the same results to several significant figures. Second, examination of the 1000-Hz ensemble shows that most of the particles are adjacent to the minimum Y^* boundary: hence, the coarseness of the grid in the Y^* direction (21 uniformly spaced points between $Y^{*,min}$ and $Y^{*,max}$) contributes to the discrepancy. This error can be reduced at the straightforward expense of adding points to the table in the Y^* direction. Third, the assumption of partial equilibrium in reactions 2–5 is not strictly correct under conditions where significant amounts of fuel are present; hence, it is responsible in part for the discrepancies between the starting and reduced schemes.

By "binning" particles, pdfs can be obtained from the steady-state ensembles. Once again, the predictions obtained using the starting and the reduced schemes are compared. For example, at 100 Hz, the reduced scheme exhibits excellent fidelity on the pdfs of temperature (Fig. 5) and of fuel mass fraction (Fig. 6). However, the pdf of Y^* is not as well-predicted. At 100 Hz (Fig. 7a), where the mean Y^* happened to agree (Fig. 4c), the pdf obtained from the reduced scheme is broader than that from the starting scheme. At 300 Hz (Fig. 7b), the discrepancy is further exaggerated. Since the rate of production of Y^* by reaction 1 is retained in the reduced scheme, the culprit is the rate of removal of Y^*; the elementary rates in the starting scheme are not reproduced in detail by the partial equilibrium submodel.

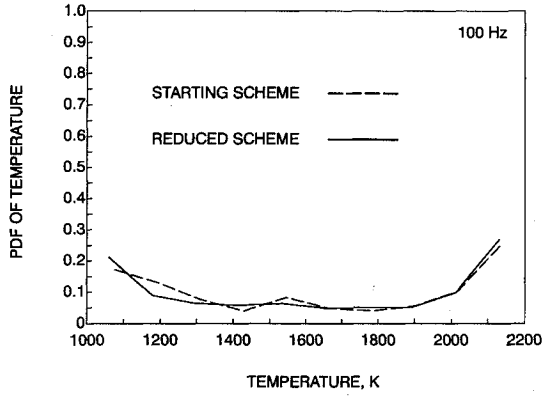

Fig. 5 Comparison of pdfs of temperature obtained from the PaSR model, using the starting and the reduced schemes. Data taken from the stochastically steady ensembles at a mixing frequency of 100 Hz.

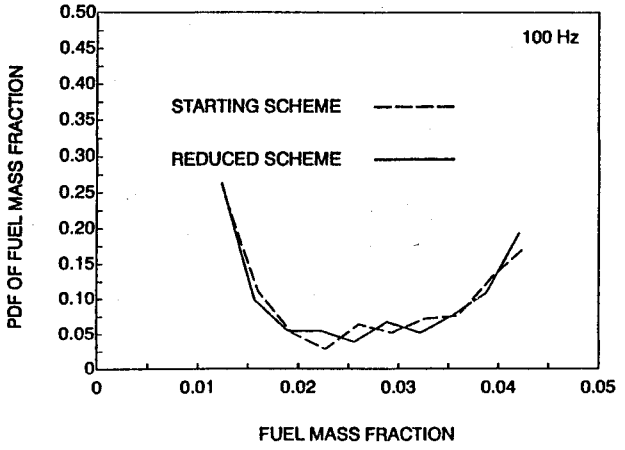

Fig. 6 Comparison of pdfs of fuel mass fraction obtained from the PaSR model, using the starting and the reduced schemes. Data taken from the stochastically steady ensembles at a mixing frequency of 100 Hz.

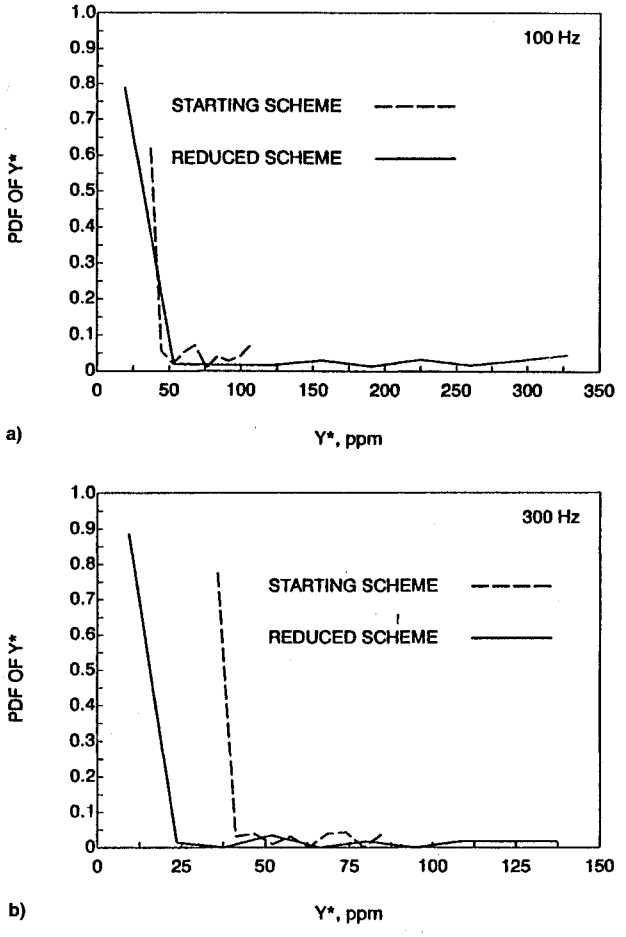

Fig. 7 Comparison of pdfs of Y^* (the combined variable based on CO and H_2 mole numbers) obtained from the PaSR model, using the starting and the reduced schemes: a) data taken from stochastically steady ensembles at 100 and b) 300 Hz.

Scatterplots of selected species and temperature can be used to show where partial equilibrium breaks down. Scatterplots were made from the stochastically converged ensembles, for both the starting scheme and the reduced scheme. The scatterplot of O atom mass fraction and temperature in the 1000-Hz ensemble (Fig. 8) shows agreement to within an order of magnitude between the two schemes, except at lower frequencies; the reason is that the particle temperatures are lower (as indicated by the means in Fig. 4a) and so reactions (2–5)

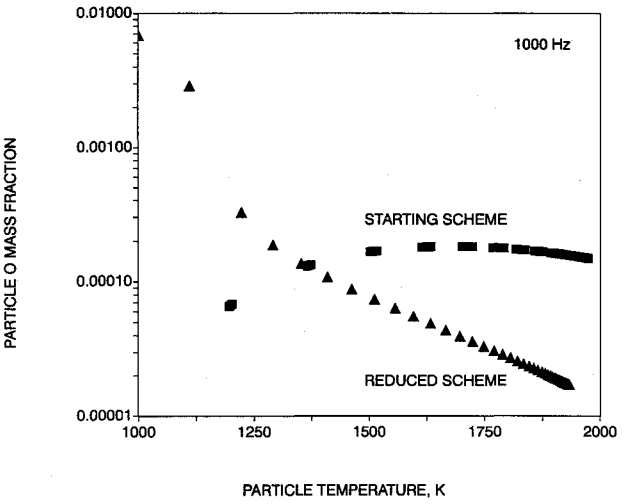

Fig. 8 Scatterplot of O atom mass fraction and temperature in the 1000-Hz ensemble; ■ = starting scheme and ▲ = reduced scheme.

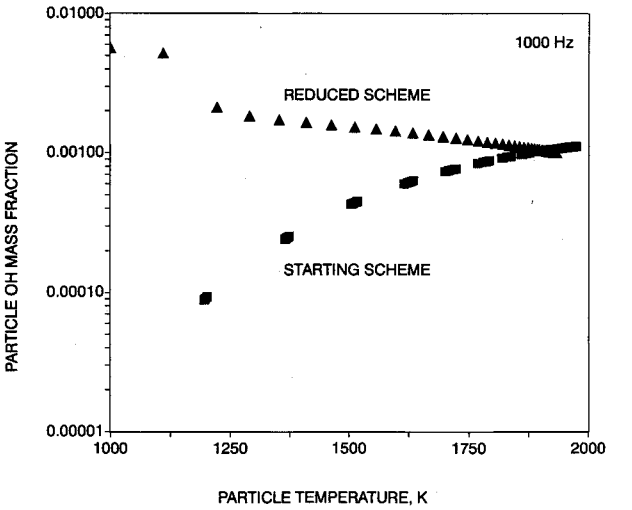

Fig. 9 Scatterplot of OH radical mass fraction and temperature in the 1000-Hz ensemble; ■ = starting scheme and ▲ = reduced scheme.

are not as fast as in hotter gases. Note that the symbols are plotted at the x-y points defined by the particle O atom mass fraction and particle temperature, respectively; since particles can lie close to each other or even coincide in this x-y space, the symbols can partially or completely overlap. The number of symbols can therefore be smaller than the number of particles (≈250). The scatterplot of OH radical mass fraction and temperature in the 1000-Hz ensemble (Fig. 9) again shows better agreement at the higher mixing frequencies and worse agreement at the lower mixing frequencies.

Detailed examination of the results along these lines shows that the error in Y^* at low frequency is caused predominantly by the partial equilibrium model, whereas that at high frequency is caused predominantly by the error in interpolation in the look-up table. Note that since both mixing and reaction contribute to the results in the scatterplots, there is some contribution from the fact that the ensemble means differ between the two schemes: 1) for O atoms the ensemble means were 154 ppm (starting scheme) and 204 ppm (reduced scheme) and 2) for OH radicals the ensemble means were 941 ppm (starting scheme) and 1281 ppm (reduced scheme).

Figure 10 shows that the molar ratio of CO to H_2 computed during autoignition and combustion of a fuel-air premixture (under the same conditions as the PaSR simulations) deviates from the partial equilibrium value. Since there is no effect of mixing in this particular calculation, it is further established

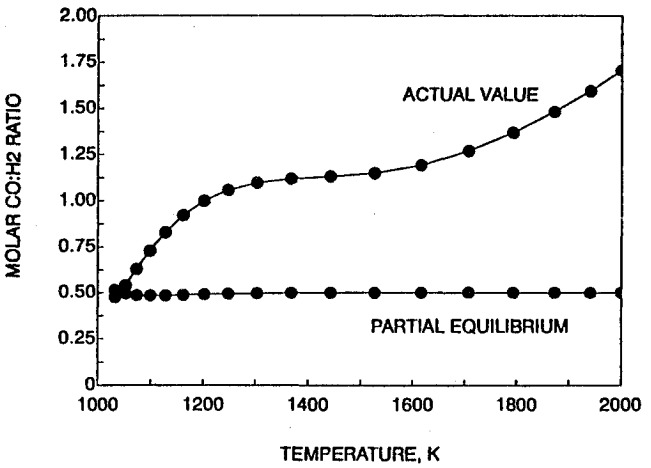

Fig. 10 Actual molar ratio of CO/H_2 compared with the partial equilibrium value, during autoignition and combustion according to the starting scheme under the same conditions as the PaSR simulations. The points are spaced by 0.5 ms.

that the assumption of partial equilibrium is a significant source of the above discrepancies.

Considering temperature (down to blowout limits), fuel mass fraction, and CO emissions, there is a reasonable degree of agreement between the reduced and the starting schemes across the range of frequencies from plug to perfectly stirred flow. Given the degree of detail in the assessment procedure, it is appropriate to conclude that the reduced scheme should be tried in multidimensional CFD studies.

VI. Conclusions

A systematic methodology for the development of combustion models for CFD has been presented, consisting of 1) qualifying a starting scheme in the PFR and PSR limits at relevant conditions, 2) reducing it to a three-variable scheme, and 3) assessing the latter by comparison with the former in the PaSR, which models turbulent reacting flow of prescribed mixing frequency, across the expected range of frequencies.

The oxidation mechanism for a complex hydrocarbon fuel—of necessity, initiated by an assumed pyrolysis step—can be reduced to a scheme requiring three variables in nonpremixed flow or two variables in premixed flow. The rate of pyrolysis is chosen to give desired results in the PFR and PSR limits; however, since this rate survives intact in the reduced scheme, any other choice can be accommodated. Partial equilibrium among CO, H_2, and radicals is assumed in order to close the thermochemical system. The reduced scheme can be directly compared with the starting scheme in the controlled and prescribed turbulence testbed provided by the Monte Carlo partially stirred reactor. The PaSR is more appropriate, for highly turbulent burners, than the traditional testbed provided by the laminar flame. The PaSR fully includes the nonlinear interaction between turbulence and chemistry. Behavior in the PaSR is identical to behavior in a single computational cell of the multidimensional Monte Carlo pdf/CFD model, which is likely to be the vehicle by which turbulence-chemistry research is transitioned to the gas-turbine combustor design community.

Under conditions representative of a gas-turbine combustor, the reduced scheme agrees extremely well with the starting scheme on the mean temperature and fuel mass fractions, and further, on the pdfs of these quantities. The mean CO and H_2 are not predicted as well, because the partial equilibrium model cannot reproduce the CO and H_2 oxidation rates of the starting scheme. The PaSR evaluations were conducted under conditions of very incomplete combustion, typical of the interior of a flame stabilization zone where significant amounts of unburned fuel exist: the partial equilibrium scheme may be expected to do better on CO and H_2 downstream of this zone.

Since NO_x formation in trace amounts does not affect the energy or minor species, NO_x emissions can be included at the straightforward expense of an additional but decoupled variable.

A three-variable reduced kinetic scheme is particularly interesting in the context of the pdf transport model for three-dimensional flows. This pdf transport equation is usually solved by a "particle-tracking" Monte Carlo method.[2,11] In this method, the particles move in three-dimensional physical ($x - y - z$) space at a rate given by the total advection operator. The tracking is conceptually identical in the present three-dimensional thermochemical ($\xi - Y_f - Y^*$) space; the same particles move in the latter space at a rate given by the mixing-plus-reaction(s) term. In both types of motion, the particle-tracking algorithm needs to interpolate the rates from a fixed grid (either the spatial grid or the tetrahedral thermochemical grid) to the present position of the particle [either $x^{(n)} - y^{(n)} - z^{(n)}$ or $\xi^{(n)} - Y_f^{(n)} - Y^{*(n)}$, respectively, for particle n]. Hence, the computational costs of these two types of tracking are similar, up to differences in the stiffness of the advection and mixing-reaction terms. In fact, since the topology of the thermochemical grid ($\xi - Y_f - Y^*$) is fixed once and for all by specification of the fuel (C_nH_m), special accelerated interpolation routines can be "hard-wired"; such speedup may not be possible for interpolation in physical space, because the CFD code must be able to handle arbitrary geometries.

Acknowledgments

This work was supported in part by the U.S. Air Force Office of Scientific Research, Bolling Air Force Base, Washington, DC, under Contract F49620-91-C-0072, Julian Tishkoff, Program Manager.

References

[1]Correa, S. M., "A Review of NO_x Formation in Gas-Turbine Combustion," *Combustion Science and Technology*, Vol. 87, 1992, pp. 329–362.

[2]Pope, S. B., "Computations of Turbulent Combustion: Progress and Challenges," *Twenty-Third International Symposium on Combustion*, The Combustion Inst., Pittsburgh, PA, 1990, pp. 591–612.

[3]Correa, S. M., and Pope, S. B., "Comparison of a Hybrid Monte-Carlo PDF/Finite-Volume Mean Flow Model with Bluff-Body Raman Data," *Twenty-Fourth International Symposium on Combustion*, The Combustion Inst., Pittsburgh, PA, 1992, pp. 279–285.

[4]Miller, J. A., and Bowman, C. T., "Mechanism and Modeling of Nitrogen Chemistry in Combustion," *Progress in Energy and Combustion Science*, Vol. 15, 1989, pp. 287–338.

[5]Correa, S. M., and Braaten, M. E., "Parallel Simulations of Partially-Stirred Methane Combustion," *Combustion and Flame*, Vol. 94, 1993, pp. 469–486.

[6]Correa, S. M., "Relevance of Non-Premixed Laminar Flames to Turbulent Combustion," *Major Research Topics in Combustion*, edited by M. Y. Hussaini, A. Kumar, and R. G. Voigt, Springer–Verlag, New York, 1992, pp. 309–338.

[7]Bilger, R. W., "The Structure of Turbulent Non-Premixed Flames," *Twenty-Second International Symposium on Combustion*, The Combustion Inst., Pittsburgh, PA, 1988, pp. 475–488.

[8]Peters, N., "Laminar Flamelet Concepts in Turbulent Combustion," *Twenty-First International Symposium on Combustion*, The Combustion Inst., Pittsburgh, PA, 1988, pp. 1231–1250.

[9]Correa, S. M., "Turbulence-Chemistry Interactions in the Intermediate Regime of Premixed Combustion," *Combustion and Flame*, Vol. 93, 1993, pp. 41–60.

[10]Chen, J.-Y., Kollmann, W., and Dibble, R. W., "PDF Modeling of Turbulent Non-Premixed Methane Jet Flames," *Combustion Science and Technology*, Vol. 64, 1989, pp. 315–346.

[11]Pope, S. B., "PDF Methods for Turbulent Reactive Flows," *Progress in Energy and Combustion Science*, Vol. 11, 1985, pp. 119–192.

[12]Borghi, R., "Turbulent Combustion Modeling," *Progress in Energy and Combustion Science*, Vol. 14, 1988, pp. 245–292.

[13]Kee, R. J., Rupley, F. M., and Miller, J. A., "Chemkin-II: A Fortran Chemical Kinetics Package for the Analysis of Gas-Phase Chemical Kinetics," Sandia National Labs., SANDIA Rept. SAND89-8009, Livermore, CA, 1989, pp. 751–757.

[14]Chen, J.-Y., and Kollmann, W., "Segregation Parameters and Pair-Exchange Mixing Models for Turbulent Non-Premixed Flames," *Twenty-Third International Symposium on Combustion*, The Combustion Inst., Pittsburgh, PA, 1990, pp. 751–757.

[15]Spalding, D. B., "Concentration Fluctuations in a Round Turbulent Free Jet," *Journal of Chemical Engineering Science*, Vol. 26, 1971, pp. 95–107.

[16]Curl, R. L., "Dispersed Phase Mixing, 1: Theory and Effects in Simple Reactors," *AIChE Journal*, No. 9, 1963, pp. 175–181.

[17]Flagan, R. C., and Appleton, J. P., "A Stochastic Model of Turbulent Mixing with Chemical Reaction: Nitric Oxide Formation in a Plug-Flow Burner," *Combustion and Flame*, Vol. 23, 1974, pp. 249–267.

[18]Pratt, D. T., "Mixing and Chemical Reaction in Continuous Combustion," *Progress in Energy and Combustion Science*, Vol. 1, 1976, pp. 73–86.

[19]Butler, G. W., "Coalescence/Dispersion Modeling of Non-Steady High Intensity Combustor Loading," AIAA Paper 85-1442, 1985.